



# Calibration strategies for elemental analysis of biological samples by LA-ICP-MS and LIBS – A review

Mauro Martinez<sup>1</sup> · Matthieu Baudelet<sup>1,2,3</sup>

Received: 7 August 2019 / Revised: 27 September 2019 / Accepted: 7 October 2019 / Published online: 8 November 2019  
© Springer-Verlag GmbH Germany, part of Springer Nature 2024, corrected publication 2024

## Abstract

Laser ablation inductively coupled plasma mass spectrometry (LA-ICP-MS) and laser-induced breakdown spectroscopy (LIBS) are widely accepted techniques for direct sampling of biological materials for elemental analysis, with increasing applications being reported over the recent years. This review is focused on the calibration materials used to quantify trace elements in different biological samples such as soft tissues (for instance brain, liver, hair) and hard tissues (bones and teeth). The design of a correct calibration strategy relies on the choice of an adapted reference material that can be commercially available or prepared in-house, which will be reviewed here. A large variety of methods has been approached and considered promising over the years, and the development of matrix-matched reference biological materials seems now closer than ever and gives hope to even better quantitation using LIBS and LA-ICP-MS.

**Keywords** Matrix-matched standards · Laser ablation · LA-ICP-MS · LIBS

## Introduction

Laser ablation inductively coupled plasma mass spectrometry (LA-ICP-MS) and laser-induced breakdown spectroscopy (LIBS) are techniques that have been increasingly used for the detection of metals and metalloids in biological samples in the last decade [1–10]. Their main advantage relies on the sampling being done by laser ablation allowing elemental analysis and chemical mapping of small areas [6, 11, 12], study the permeation of drugs [8, 13–15], element accumulation [4, 15–17], nanoparticle interaction with cells [18, 19] and other biological samples [18], to mention few of them. LA-ICP-MS and LIBS have been complementary techniques that

provide important chemical information in quasi-real time, opening a new field in elemental bio-imaging. When the former has shown its capabilities for the analysis of traces and minor, LIBS is a lot more versatile when elements of interest are majors and minors, especially when these are N, O, and H. Even new approaches using LIBS provide easier protocols for the analysis of halogens via molecular emission in the plasma. The samples and matrices of interest cover a large spectrum, from human and animal soft tissue (skin, brain, liver, lungs, hair [6, 11, 20–22]) and hard tissues (bones, cartilage, and teeth [23–27]).

Nevertheless, as any analytical technique, high accuracy is dependent on the calibration strategy used for the analysis. This calibration strategy is the combination of the calibration procedure and calibration method used. In order to compensate instrument drifts, instabilities, and matrix effect on the plasma, the internal standard (IS) method is the most common calibration method used in LA-ICP-MS and LIBS [16, 28, 29]. Nonetheless, external calibration [28], standard addition [30], or multivariate analysis [31–33] are also used. The element or isotope used as the internal standard is usually an element that is a major constituent of both the sample and the calibration material, considering its concentration to be constant in all cases. Consequently, the calibration procedure for the analysis is going to have the greatest impact on the accuracy of the concentration values. The calibration

---

Published in the topical collection *Young Investigators in (Bio-) Analytical Chemistry* with guest editors Erin Baker, Kerstin Leopold, Francesco Ricci, and Wei Wang.

---

✉ Matthieu Baudelet  
baudelet@ucf.edu

<sup>1</sup> National Center of Forensic Science, University of Central Florida, 12354 Research Parkway #225, Orlando, FL 32826, USA

<sup>2</sup> Chemistry Department, University of Central Florida, Physical Sciences Bld. Rm. 255, 4111 Libra Drive, Orlando, FL 32816, USA

<sup>3</sup> CREOL – The College of Optics and Photonics, University of Central Florida, 4304 Scorpious St, Orlando, FL 32816, USA

procedure is known as the set of operations which establishes, under specified conditions, the relationship between the signal from the analytical instrument and the corresponding values of concentration for an analyte [34]. These specific conditions are the key, and it is possible to group within these conditions the sample treatment, the calibration material, and the instrumental conditions to obtain the signal.

The International Union of Pure and Applied Chemistry (IUPAC) defines a calibration material as a material of known composition or properties which can be presented to the analytical instrument for calibration purpose [34]. In an analysis by atomic absorption spectroscopy (AAS), ICP-optical emission spectroscopy (ICP-OES), and ICP-MS, so much effort is spent on the sample treatment to become similar to the calibration material, i.e., digesting and diluting the sample solution with the same density and concentration range as the calibration solution. The advantage of diluted solutions relies in their reproducible transportation, nebulization, droplet selection, droplet transportation, and atomization/ionization. In contrast, direct solid analysis by LA-ICP-MS and LIBS makes the controlled transformation of the sample into a similar calibrated dry aerosol much more difficult. This is due to the difficulties in matching the properties of the dry aerosols produced by an unknown solid sample and those from a calibration material. In order to correlate the instrumental signal between the calibration material and the sample, it is imperative to tune the laser ablation conditions so the same mass is removed, the particle size distribution on the aerosols and their transport to the torch will be similar, as well as the plasma properties in the case of LIBS. Otherwise, the concentration deduced from the non-matching standard will not be accurate. In addition, to reproducing the laser ablation conditions, two properties need to be respected by the calibration material:

1. Chemical similarity, so the major component of the matrix can be the same for normalization.
2. Similar mechanical and optical properties, to reproduce the same laser-matter interaction during the ablation.

As a result, having access to such calibration material is the Holy Grail in LA-ICP-MS and LIBS when quantitative analysis is required. Respecting the above conditions lead to the creation of a matrix-matched calibration material. Such materials are either commercially available or made in-house. This paper reviews the different strategies used in the published literature and will discuss potential ameliorations for better analytical performances of laser-ablation-based techniques.

## Commercial reference materials

Presently, few commercial certified reference materials (CRM) exist that have been used for LA-ICP-MS and

LIBS (Table 1) for the analysis of biological materials. Traditionally, these CRM are used as validation materials for either AAS, ICP-OES, or ICP-MS, although they come as a powder or lyophilized powder, which can be seen as inconvenient in many cases for LA-ICP-MS and LIBS.

Narukawa et al. [30] determined trace element content in biological tissues by LA-ICP-TOF-MS. They prepared the sample as a dried deposit of solubilized biological tissue after a treatment with formic acid. With this strategy, they created a uniform film from a dry slurry of the original material. Using CRMs RM8414, DORM-3, DOLT-4, SRM2976, and SRM15566b with a subsequent same treatment, they built standard addition calibration curves using CRM TORT-2 as a validation material and interestingly a whey-based protein powder as their blank material while rhodium (Rh) was chosen as the internal standard, containing this in the formic acid solution. Very good linear calibration curves and limits of detection (LOD) were obtained (1, 2, 6, 0.2, and 0.05  $\mu\text{g}\cdot\text{g}^{-1}$  for Mn, Cu, Zn, Cd, and Pb respectively). In addition, they showed a low elemental fractionation for spot size above 350  $\mu\text{m}$ , which is large for LA-ICP-MS. A disadvantage for this strategy is the dynamic range of concentrations being limited by the CRM used.

Using a different strategy, Monk et al. [35] introduced the use of pelletized CRMs to follow the isotopic ratio of Zn and Cu by Cryo-LA-ICP-TOF-MS, and applied this methodology for the analysis of a dissected worm. The CRMs were pressed with 25 tons of pressure without using any binder. To optimize a low elemental fractionation with these calibration samples, they used a 100- $\mu\text{m}$ -laser spot size, 2.6 mJ of laser power and  $-10^\circ\text{C}$  in the cryogenic chamber. Because of the rapid analysis time and spatial resolution, they could identify variations in the metal tissue storage at the sub-mm scale, although with LOD of 21.4 and 78.4  $\mu\text{g}\cdot\text{g}^{-1}$  for Zn and Cu respectively.

Using the similar strategy of pressed powder pellets, Noél et al. [5, 38] characterized the kinetics of copper, zinc, and mercury after exposure of wild and captive grizzly bears using hair as the sample and LA-ICP-MS as the analytical technique. Dogfish liver powder (CRM DOLT-2) was chosen over human hair powder CRM (IAEA-085 and IAEA-086) because the pellets showed better mechanical properties. Furthermore, DOLT-2 was still being certified for the elements of interest and homogeneous as a pressed pellet without using a binder. Sulfur was chosen as the internal standard due to its high constant signal across the length of the hair (while the concentration was not measured but evaluated from the literature), although no information was provided about it for the CRM DOLT-2 and the authors had to measure it independently. All hairs were ablated at a spot size of 30  $\mu\text{m}$ , a speed of 50  $\mu\text{m}\cdot\text{s}^{-1}$ , frequency of 20 Hz and fluence of  $12.0 \pm 1.9 \text{ J}\cdot\text{cm}^{-2}$ , while the CRM was ablated at a spot size of 100

**Table 1** Commercial reference materials used for LA-ICP-MS and LIBS

Code	Description	Physical state	Element	LOD ( $\mu\text{g}\cdot\text{g}^{-1}$ )	Ref.
NRCC RM8414	Bovine muscle (Beef)	Powder	Mn	1	[30, 35]
NIST SRM1566b	Oyster tissue	Powder	Cu	2	
NIST SRM2976	Mussel tissue (trace elements and methylmercury)	Powder	Zn	6	
NRCC DORM-3	Fish protein-certified reference material for trace metals	Powder	Cd	0.2	
NRCC TORT-2	Lobster hepatopancreas reference material for trace metals	Powder	Pb	0.5	
			Zn	21.4	
			Cu	78.4	
NIST SRM397	Human hair	Powder	Cr		[24]
			As		
			Hg		
			Sb		
			Pb		
NIST SRM1486	Bone meal, trace element	Powder	Zn		[9, 24, 36]
			Sr		
			Cd		
			Pb		
			Cr		
			As		
			Hg		
			Sb		
NIST SRM1400	Bone ash, trace element	Powder	Sr		[37]
			Fe		
			Pb		
			K		
			Zn		
NRCC DOLT-4/DOLT-5	Dogfish liver-certified reference material for trace metals	Powder	Hg	0.09	[5, 17, 30, 35, 38]
			Ca	30	
			Cu	0.1	
			Zn	0.1	
			Pb	0.04	
			Cd	0.21	
			Fe	32	
NIST SRM610-616	Series for trace element in glass	Pellet	Sr		[17, 39, 40]
			Na		
			Mg		
			K		
			Ca		
			Mn		
			Zn		
			Rb		
			Ba		

$\mu\text{m}$ , speed of  $10\mu\text{m s}^{-1}$ , frequency of 5 Hz, and fluence  $7.2 \pm 0.8\text{J cm}^{-2}$ . LODs of 32, 0.81, 1.3, 0.21, 0.09, and  $0.01\mu\text{g}\cdot\text{g}^{-1}$  for Fe, Cu, Zn, Cd, Hg, and Pb respectively were obtained and RSD ranged from 5.8 to 7.3% for all elements analyzed except for Pb, which had a RSD value up to 20.9%. This high RSD for Pb was associated to the concentration ( $0.22\mu\text{g}\cdot\text{g}^{-1}$ ) being close to the LOD, even if it was 22 times higher than the calculated LOD. Nonetheless, a major flaw in the calibration strategy resided in the difference of LA-ICP-MS operational parameters between the CRM and the samples and the authors noticed a major issue, which was the underestimation of the concentration by LA-ICP-MS when compared with ICP-MS. Later, Christensen et al. [17] followed the same strategy to study how zinc deficiency played a greater role than lead in the demise of the Franklin Expedition. In order to improve the

measurement of Pb, they used the NIST glass SRM 613, and CRM DOLT 2 for Cu and Zn following the same protocol as Noël et al. [5, 38]. Same underestimation issues were noticed leading to challenges for a quantitative discussion.

Stadlbauer et al. [24] attempted to verify the authenticity of Mozart's skull by analyzing bones, teeth, and hair from individuals from 18th/19th centuries by LA-ICP-MS. Hair analysis was performed using the hair powder NIST SRM 397 pressed into a pellet using polyethylene as a binder. Bones and teeth hydroxyapatite (HA) powders were spiked with Pb, Cr, Hg, As, and Sb, and then pelletized. A pellet from the bone meal NIST SRM 1486, a separately prepared HA sample, and a modern bone were characterized by ICP-MS to be used as reference sample to validate the calibration curve with a recovery varying between 92 and 111%. The

results showed that the old individuals presented levels of Pb and Sb respectively ten and three times higher than modern individuals showing a possible exposure to heavy metals.

A collection of CRM samples that is often used is the NIST glass series SRM 610–616. They were involved in the quantification of metal content in otolith [40, 41] and coral [39] by LA-ICP-MS. In these cases, the CRM series is either used to build a single-point calibration curve or using Ca signal as the IS [39–41]. This choice of CRM has been used to optimize the aerosol size distribution and their transportation to the ICP torch to maximize the signal response while avoiding the elemental fractionation during the ablation. All CRMs described above have been used in different applications for a quantitative purpose. The main hypothesis these studies rely on was that the ablation conditions would be comparable between the standards and the samples. However, this can only be confirmed in few cases [30]. None of them presents any detail or argument about matching the mass removal, the aerosol size distribution, and their transportation to the plasma source in the case of LA-ICP-MS. The chemical similarity is also questioned in some studies (to the extreme case of comparing glass and hair) and Fig. 1 summarizes these choices of standards for different biological materials.

Furthermore, the concentration range and the number of elements that could be quantitatively evaluated were limited. To improve the calibration strategy for a wider range of biological samples by LA-ICP-MS and LIBS, several authors have chosen to prepare themselves a set of calibration materials adapted to their study while being matrix-matched. Some innovative strategies for calibration using in-home matrix match material have been summarized in Table 2 and discussed in the next section.

## Matrix matching by in-house prepared calibration material

### Soft tissue

One of the calibration strategies with in-house prepared calibration materials (PCM) for LA-ICP-MS is the spiking of the equivalent homogenized tissue followed by further homogenization. Then, this spiked material is frozen, cryo-cut into slices, and mounted on glass slides. To determine the concentration in the PCM, replicates are digested with acid and analyzed by Pneumatic Nebulization-ICP-MS (PN-ICP-MS) [6, 11, 20, 55, 56]. This procedure is not simple to perform, and implies the incorporation of a cryogenic apparatus in the laser ablation chamber. If the sample is a native tissue, it needs to be properly preserved and treated before grinding. Furthermore, it is assumed that the standards and the sample have a similar chemical composition, compensating for fractionation effects. This calibration strategy is normally used

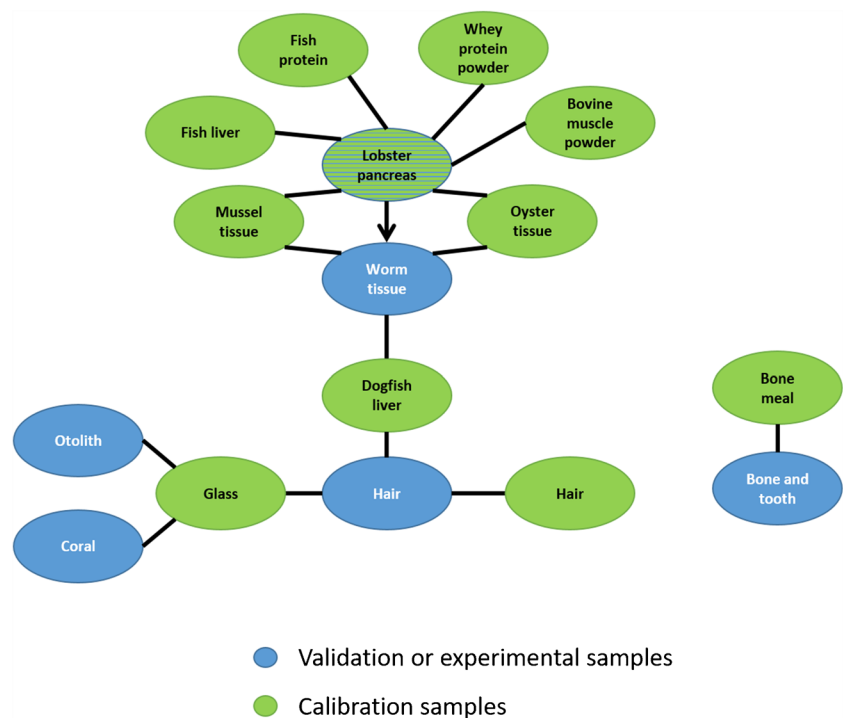
to quantify the elemental distribution of tissue cross sections such as brain [6, 11, 55], liver [20], and cancerous tissues [2] to mention few of them. To improve this calibration strategy, Pozebon et al. [6] reported the use of a pneumatic nebulizer to partially desolve the aerosols, reducing polyatomic ion formation and increasing sensitivity. Also, it was observed that the sensitivity of LA-ICP-MS and the linearity of the calibration curves generally improved when the ablated aerosol (from the solid homogenate of mouse brain tissue fixed on a glass slide) was introduced into the plasma torch together with the aerosols produced by nebulization of 2% (v/v) HNO<sub>3</sub>.

This procedure was approached as well on LIBS analysis. Ahmed et al. [42, 57] show that immersing excised thyroids in iodine (I) and lithium (Li) solution could benefit the determination of these elements on this tissue. On a first approach, the excised thyroids were immersed in 0, 0.28, 0.37, 0.55, or 1.10 µg.g<sup>-1</sup> Li solutions for 24 h at room temperature. After immersion, the thyroids were rinsed with saline solution and immersed in liquid nitrogen for several seconds followed by 24-h storage in -80 °C before performing LIBS. After running the calibration curve, a LOD of 0.12 µg.g<sup>-1</sup> of Li of this kind of tissue was estimated [57]. Another use of this methodology was the evaluation of the interchange of I in the thyroid by LIBS [42].

Another interesting calibration strategy is the use of inkjet solution, spiked with elements of interest, to be printed on paper in patterns that can be analyzed by LA-ICP-MS [43, 44]. As a first evaluation, Bellis et al. [43] reported the use of line patterns printed with commercial cyan inkjet solution, adjusting the density levels (20%, 40%, 60%, 80%, and 100% (i.e., no transparency)) to control the amount of ink by line. In addition, an inline solution nebulization was used to introduce the internal standard simultaneously. The method developed here showed a spatial resolution of at least 100 µm. The figures of merit of this calibration strategy were unfortunately not studied in details. Nevertheless, Bonta et al. [44] reported a similar application printing cyan inkjet solution, comparing different types of papers. This work included the addition of a gold film to be used as an internal standard. The patterns printed on paper using inkjet printer were 400 µm<sup>2</sup>, in different print density settings (100, 75, 50, and 25%). The patterns were printed with cyan ink, which contains an organic copper complex providing a blue color. They were then mounted on glass slides and gold-coated for 30 s. The authors could demonstrate that the use of gold as the internal standard was successful, accounting for instrumental drifts and ablation fluctuations due to the inhomogeneity of the patterns. The authors applied this calibration strategy for the chemical imaging of Cu in peony petals.

An alternative calibration strategy was presented by Stärk et al. [45] using a thin layer of spiked agarose gel as PCM for LA-ICP-MS. In this procedure, agarose was dissolved with a sodium acetate solution and spiked with a multi-elemental solution. Buffering was also required to counter the acidity

**Fig. 1** Summary of the types of commercially available CRM matrices for the analysis of biological materials in the literature



of the multi-elemental solution. The agarose solutions were mounted on a glass slide for the analysis. The film thickness was around 30  $\mu\text{m}$  with a RSD of 8% and the recovery from the elements ranged between 90 and 110%. This research was focused on the toxicology of tungsten carbide and tungsten carbide–cobalt nanoparticles used in incubation experiments. Because of the wide range of biological specimen studied, a considerable variation in the concentrations was found but the results in comparison with PN-ICP-MS were concurrent. Unfortunately, there was no CRM available to enable checking of the accuracy of the analytical method by direct comparison. Turková et al. [46] moved forward with this calibration strategy studying metal accumulation in tapeworm cross sections using LA-ICP-MS. Synthetic matrix-matched materials containing Fe, Pb, and Zn were prepared by spiking an agarose gel using the similar procedure with a recovery rate between 82 and 117%. Carbon  $^{12}\text{C}^+$  was used as the internal standard isotope to correct for the different tissue density and absorption rates. It was also tested under different fluence values, observing that above 2  $\text{J}\cdot\text{cm}^{-2}$ , the film was ablated through as well as the glass slide underneath. The prepared set of multi-elemental agarose gel standards was used for the quantitative elemental mapping of cross-sections of *Hymenolepis diminuta* embedded in paraffin. They showed that using a 193 nm ArF laser coupled to ICP MS, they could achieve LODs of 8.7, 0.57, and 0.07  $\text{mg}\cdot\text{kg}^{-1}$  for Fe, Zn, and Pb, respectively. The content of Zn, as a biogenic element, was homogeneously distributed within the cross section, primarily in reproductive structures, while the Pb elemental distribution was found to be more concentrated in the surface.

Vanhaecke et al. [20, 47, 48] introduced another use of the gelatin films as calibration material for LA-ICP-MS. A 10% (w/v) gelatin solution was prepared and spiked with the elements of interest. A micro-volume from this solution was mounted on a glass slide for analysis while the remaining of the solution was validated by PN-ICP-MS to quantify the recovery. This procedure was applied to map the Br distribution in rat lungs [47], Pt after administration of chemotherapy drugs [48], and Cu in rat livers [20]. LA-ICP-MS was evaluated as an alternative to radioluminography (RLG) to assess the distribution of a novel anti-tuberculosis compound containing bromine as a “hetero-element” and its metabolites over the organs of a rat. After administration of the Br-containing drug and enough time to allow drug uptake and distribution, the sacrificed animal was frozen and embedded in carboxymethyl cellulose, after which thin sections were obtained using a microtome. The LOD for Br was estimated to be 0.1  $\text{mg}\cdot\text{g}^{-1}$ , which is sufficiently low to allow visualization of Br in the main organs of interest. In the second work listed, LA-ICP-MS was employed for the quantification of platinum in tissue samples of rats with peritoneal carcinomatosis, receiving intraperitoneal treatment with the Pt-containing chemotherapeutic drug oxaliplatin, and in the perfusate solution used for this purpose. LOD obtained for platinum in tissue samples was 0.25  $\text{ng}\cdot\text{g}^{-1}$  and a recovery of  $99 \pm 3\%$ . To establish further confidence in the approach used for quantifying the  $^{195}\text{Pt}$  distribution in each tumor, a neighboring thin section was digested and the total  $^{195}\text{Pt}$  concentration via PN-ICP-MS. The values obtained were generally in good agreement with the  $^{195}\text{Pt}$  distribution profiles generated by LA-ICP-MS, considering the lack of CRM for this specific

**Table 2** In-house matrix-matched reference materials used for LA-ICP-MS and LIBS

Sample	Matrix-match standard material	Elements	LOD	Ref.
Soft tissue	Spiking of the equivalent homogenized tissue followed by further homogenization	Li	0.12 $\mu\text{g.g}^{-1}$	[42]
Soft tissue	Ink-jet solution spiked with elements of interest and printed as patterns on paper	Cu		[43, 44]
Soft tissue	Spiked agarose gel	Co	5 $\text{pg mm}^{-2}$	[46]
		Fe	27 $\mu\text{g.g}^{-1}$	
		Zn	5.2 $\mu\text{g.g}^{-1}$	
		Pb	0.31 $\mu\text{g.g}^{-1}$	
Soft tissue	Gelatin solution was prepared and spiked with the elements of interest	Br	0.1 $\mu\text{g.g}^{-1}$	[47]
		Pt	0.25 $\text{ng.g}^{-1}$	[48]
		Cu	1.5 $\mu\text{g.g}^{-1}$	[20]
		Pt	8 $\text{ng.g}^{-1}$	[49]
Soft tissue	Egg yolk spiked with the elements of interest	Th	2.2 $\text{ng.g}^{-1}$	[50]
Soft tissue	Epoxy mixtures as standard support	Gd	0.13 mM	[51]
		Si	0.06 mM	
		Na	0.20 mM	
		Fe	0.21 mM	
Hair	Hair spiked with the elements of interest	Pb		[16]
Hair	Doped keratin films	Pb	82 $\text{ng.g}^{-1}$	[52]
Bone and teeth	Co-precipitation of hydroxyapatite spiked with the elements of interest	Cd	1.4 $\text{ng.g}^{-1}$	[53]
		Al	751 $\text{ng.g}^{-1}$	
Bone and teeth	Calcium oxalate ( $\text{CaC}_2\text{O}_4$ ) spiked and pressed on a pellet	Cu	9 $\mu\text{g.g}^{-1}$	[54]
		Mg	8.5 $\mu\text{g.g}^{-1}$	
		Zn	10 $\mu\text{g.g}^{-1}$	
		Sr	17 $\mu\text{g.g}^{-1}$	
Bone and teeth	Co-precipitation of hydroxyapatite spiked with the elements of interest and pellet sintered to increase hardness and density	Co	49 $\mu\text{g.g}^{-1}$	[27]
		Mn	130 $\mu\text{g.g}^{-1}$	
		V	55 $\mu\text{g.g}^{-1}$	
		Ni	42 $\mu\text{g.g}^{-1}$	
		Sr	21 $\mu\text{g.g}^{-1}$	

application. This confirms the utility of the gelatin-based standards for quantitative mapping of the Pt distribution in biological tissue sections. The third work compared the performance of the gelatin PCM with the spiked homogenized tissue section mentioned above. In this case, the LOD were comparable, 1.5  $\text{ng.g}^{-1}$  and 0.7  $\text{ng.g}^{-1}$  of Cu respectively. The calibration curves were statistically comparable as well. This led to the conclusion that a calibration material based on spiked gelatin droplets can be recommended for quantitative LA-ICP-MS thanks to its versatility, simplicity, low cost, and large range of possible concentrations.

Gelatin film as a calibration material has some advantage over the other strategies discussed. Using the same protocol to prepare the spiked gelatin, some studies have frozen it and cut it with a cryotome to create slides for posterior analysis [4, 13, 49]. Niehaus et al. [49] have focused on the aerosol characterization and the fractionation effects for slides of cryogenized gelatin and Technovit (poly-2-hydroxyethyl methacrylate) as PCM for LA-ICP-MS. One of the first conditions we mentioned is that the laser ablation must behave similarly for the matrix-matched PCM and the sample. This work presented a careful study of the aerosols produced by laser ablation using an optical particle counter inserted in-line between the LA and the ICP-MS,

while helium served as the carrier gas for material transport. Technovit produced a considerably large number of particles above 0.3  $\mu\text{m}$  while the gelatin aerosols were mostly in the lower nanometer range. The diameter of the aerosols increased with the ablation laser fluence to millimeter-sized particles for both materials. Ionization efficiency in the ICP torch was similar for both gelatin-based aerosols and traditional liquid aerosols, the vaporization of gelatin particles requiring more time. Additionally, fractionation during the ablation process (at different fluences) in gelatin was studied by recording the isotope ratios of standards spiked with Ti and V. The results indicated a strong deviation of up to 20% from the expected  $^{51}\text{V}/^{48}\text{Ti}$  ratio for laser fluences close to the ablation threshold, confirming a non-stoichiometric sampling. Nonetheless, it was not clear if this behavior can be extrapolated to real samples. Technovit [15] and 2-hydroxyethyl methacrylate (HEM) [58] have been reported as media to spike with elements of interests with LOD of 30  $\text{ng.g}^{-1}$  and 8  $\text{ng.g}^{-1}$  of Pt respectively.

In a similar strategy, Reifschneider et al. [14] matrix-matched PCM based on egg yolk were prepared. With an egg yolk separated carefully by collection with a syringe, for each calibration material, 800 mg of the mixture of three different egg yolks was spiked with 200  $\mu\text{L}$  of the respective

thallium standard solution. After spiking, the mixture was homogenized and shaken for 1 h carefully to avoid the formation of bubbles, which may negatively influence the homogeneity of the prepared material. After homogenization, the viscous homogenate solution was heated to a temperature of 90 °C for 10 min and was allowed to cool down in order to generate a solid structure similar to tissue. After cooling down, the solid blocks were removed from the vial and embedded in NEG 50 before sectioned using a cryogenic microtome. The calibration material showed an excellent homogeneity and a good linearity with low LOD 2.2 ng.g<sup>-1</sup>.

Additionally, the use of epoxy mixtures as standard support was reported by Sancey et al. [51]. On this case, the samples were then embedded in EPON (1:1 mixture of diglycidyl ether and dodecylsuccinic anhydride, density of 1.22 g/L). The sample surfaces were prepared using a microtome. To allow for elemental quantification, standards containing elements of known concentrations were embedded in the same EPON resin. CH<sub>3</sub>COONa, (CH<sub>3</sub>COO)<sub>2</sub>Fe, and AGuIX® were used as standards for Na, Fe, Gd, and Si, respectively, at 5 concentrations ranging from 1 to 40 mM. The powders were mixed with the resin (for a minimum of 4 h), warmed for 2 days (60 °C), and finally prepared using a microtome. The calibration measurements yielded LOD estimates for Gd, Si, Na, and Fe of 0.13, 0.06, 0.20, and 0.21 mM, respectively. This methodology was applied to study the distribution of elements listed before on kidney rats via high-resolution imaging by LIBS.

## Hair

The first idea to create a reference material for hair analysis has been the immersion of hair in a solution with the element of interest at given concentrations [59–61]. Dressler et al. [60] reported the sample throughput is high and the LODs of trace elements are from microgram per gram to nanogram per gram range. It was demonstrated that the proposed method could be applied to measure the concentration of elements in different types of hair, either human or animal. Nonetheless, the LODs are highly dependent on the intrinsic concentration of each element in the hair to be used as a PCM.

Other studies preferred the direct comparison of the same pool of hairs by characterizing the metal content by PN-ICP-MS for a subset and the rest by LA-ICP-MS [16, 62, 63]. However, hairs are known to be heterogeneous, showing a longitudinal variation in their elemental profile with growth. This heterogeneity only allows a comparison with an average concentration for the hair. In fact, Bartkus et al. [16], while reporting coefficients of determination between 0.93 and 0.97, showed a high RSD in the signal when both were compared. Similar results were reported by Byrne et al. [62] and Steely et al. [63]

An innovative calibration strategy for hair analysis by LA-ICP-MS is presented by Cheajesadagul et al. [52], where

doped keratin films are used as calibration materials for the determination of Pb along hair strands. They compared with the strategy of soaking hair in a solution with the element of interest. The procedure to prepare the keratin films includes the extraction of this protein from human hair by the “Shindai method,” obtaining at the end a solution rich in keratin. Films were formed by self-assembly, self-aggregation, and cross-linking activities of keratin protein with trichloroacetic acid (TCA). Keratin film doped with Pb showed better recovery and linearity than the soaked hair strand. As hair strands might have limited surface area for Pb adsorption and not the right physiology to retain it, they are not able to retain high quantities of Pb on hair surface, whereas keratin films are able to do so. For Pb quantification in this application, a LOD of 82 ng g<sup>-1</sup> was reported.

## Bones and teeth

The quantitative analysis of bones and teeth has been done using calcium-rich compounds, such as hydroxyapatite (HA) or calcium carbonate, either commercially available or synthesized, as matrix-matched PCM [26, 28, 53, 64–69]. Ugarte et al. [53] presented a calibration material containing twelve analytes (Mg, Al, V, Mn, Zn, As, Sr, Rb, Cd, Ba, Hg, and Pb). They prepared HA by co-precipitation of hydroxyapatite from calcium nitrate tetrahydrate (CaNO<sub>3</sub> 4H<sub>2</sub>O) and ammonium dihydrogen phosphate (NH<sub>4</sub>H<sub>2</sub>PO<sub>3</sub>), obtaining a Ca/P ratio similar to the real sample. Once synthesized, the concentration of the analytes in the standards was carefully determined while recoveries for the analytes were highly dependent on the element. The hydroxyapatite standards were found to be homogeneous and provided a linear calibration curve (coefficients of determination were better than 0.991 for most analytes). Limits of detection were estimated between 1.4 ng g<sup>-1</sup> for Cd and 751 ng g<sup>-1</sup> for Al. The measured values for Mg, Zn, Sr, and Pb in pelletized SRM 1486 Bone Meal were in good agreement with the CRM values. This HA synthesis methodology was followed by other authors as the best approach to mimic tooth composition [26, 28, 65]. However, although the pelletized HA powder has a consistent elemental composition with the calcified material, the ablation of its surface can have a different behavior due to density and compaction mismatch with the sample.

Another approach for this kind of samples is shown by Singh et al. [54] using calcium oxalate (CaC<sub>2</sub>O<sub>4</sub>) spiked and pressed on a pellet as calibration methodology to determine Cu, Mg, Zn, and Sr on kidney stone samples. On this case, the CaC<sub>2</sub>O<sub>4</sub> was spiked with the elements of interest solutions to obtain a pellet with a range of concentration between 50 and 5000 µg g<sup>-1</sup>. After running the calibration curve, a LOD of 9 µg g<sup>-1</sup>, 8.5 µg g<sup>-1</sup>, 10 µg g<sup>-1</sup>, and 17 µg g<sup>-1</sup> for Cu, Mg, Zn, and Sr, respectively, was estimated.

Martinez et al. [27] expanded this latter approach for the synthesis of matrix-matched materials to analyze calcified samples by LIBS. In this work, HA synthesis is similar with Ugarte et al. [53], with the inclusion of a sintering process after the HA powder was pelletized. During the sintering process at 1200 °C, the HA goes through compaction and densification, forming a hard material with a high density [70]. Following this procedure, the ablation on the material surface was similar to the one on tooth samples. These ceramic materials showed good homogeneity. LOD of 49  $\mu\text{g g}^{-1}$ , 130  $\mu\text{g g}^{-1}$ , 55  $\mu\text{g g}^{-1}$ , 42  $\mu\text{g g}^{-1}$ , and 21  $\mu\text{g g}^{-1}$  for Co, Mn, V, Ni, and Sr, respectively, were attainable in their LIBS conditions. They compared the Sr concentration values for teeth cross sections with a bulk analysis of the same section by dilution ICP-MS, showing a very good agreement between the LIBS and ICP-MS results. This methodology showed the potential to synthesize a good matrix-matched reference material reproducing the LA behavior of the sample under study.

## Conclusion

Through this review of different calibration strategies, striking innovations have played a constructive role towards chemically, mechanically, and optically similar reference materials for laser ablation. The mimic on the chemical structure, hardness, and density is really important to obtain a similar mass removal, particle size distribution, transport, and atomization/ionization in a matrix-matched reference material for LA-ICP-MS; in addition, similar plasma conditions (densities and temperature) for LIBS are required. Chemical similitude is usually achieved but differences in hardness and density still pose a challenge. While applications such as drug interaction and bioaccumulation drive the need for quantitative elemental analysis in biological samples, more fundamental research is needed to rapidly obtain good matrix-matched reference materials that will catapult the use of LA-ICP-MS and LIBS as reference quantitative techniques for biological analysis in fields such as forensics, medicine, archaeology, and anthropology.

## Compliance with ethical standards

This critical review did not involve human participants and/or animals.

**Conflict of interest** The authors declare that they have no conflict of interest.

## References

- Bauer OB, Hachmöller O, Borovinskaya O, Sperling M, Schurek H-J, Ciarimboli G, et al. LA-ICP-TOF-MS for rapid, all-elemental and quantitative bioimaging, isotopic analysis and the investigation of plasma processes. *J Anal At Spectrom.* 2019. <https://doi.org/10.1039/c8ja00288f>.
- González de Vega R, Fernández-Sánchez ML, Pisonero J, Eiró N, Vizoso FJ, Sanz-Medel A. Quantitative bioimaging of Ca, Fe, Cu and Zn in breast cancer tissues by LA-ICP-MS. *J Anal At Spectrom.* 2017;32(3):671–7. <https://doi.org/10.1039/c6ja00390g>.
- Busser B, Moncayo S, Trichard F, Bonnetterre V, Pinel N, Pelascini F, et al. Characterization of foreign materials in paraffin-embedded pathological specimens using in situ multi-elemental imaging with laser spectroscopy. *Modern Pathol: an official journal of the United States and Canadian Academy of Pathology, Inc.* 2017. <https://doi.org/10.1038/modpathol.2017.152>.
- Birka M, Wentker KS, Lusmoller E, Arheilger B, Wehe CA, Sperling M, et al. Diagnosis of nephrogenic systemic fibrosis by means of elemental bioimaging and speciation analysis. *Anal Chem.* 2015;87(6):3321–8. <https://doi.org/10.1021/ac504488k>.
- Noel M, Spence J, Harris KA, Robbins CT, Fortin JK, Ross PS, et al. Grizzly bear hair reveals toxic exposure to mercury through salmon consumption. *Environ Sci Technol.* 2014;48(13):7560–7. <https://doi.org/10.1021/es500631g>.
- Pozebon D, Dressler VL, Mesko MF, Matusch A, Becker JS. Bioimaging of metals in thin mouse brain section by laser ablation inductively coupled plasma mass spectrometry: novel online quantification strategy using aqueous standards. *J Anal At Spectrom.* 2010;25(11):1739. <https://doi.org/10.1039/c0ja00055h>.
- Romaris-Hortas V, Bianga J, Moreda-Pineiro A, Bermejo-Barrera P, Szpunar J. Speciation of iodine-containing proteins in *Nori* seaweed by gel electrophoresis laser ablation ICP-MS. *Talanta.* 2014;127:175–80. <https://doi.org/10.1016/j.talanta.2014.04.003>.
- Bianga J, Bouslimani A, Bec N, Quenet F, Mounicou S, Szpunar J, et al. Complementarity of MALDI and LA ICP mass spectrometry for platinum anticancer imaging in human tumor. *Metallomics: integrated biometal science.* 2014;6(8):1382–6. <https://doi.org/10.1039/c4mt00131a>.
- Hare D, Austin C, Doble P, Arora M. Elemental bio-imaging of trace elements in teeth using laser ablation-inductively coupled plasma-mass spectrometry. *J Dent.* 2011;39(5):397–403. <https://doi.org/10.1016/j.jdent.2011.03.004>.
- Curtin P, Austin C, Curtin A, Gennings C, Arora M, Tammimies K, et al. Dynamical features in fetal and postnatal zinc-copper metabolic cycles predict the emergence of autism spectrum disorder. *Sci Adv.* 2018;4(5):eaat1293. <https://doi.org/10.1126/sciadv.aat1293>.
- Feng L, Wang J, Li H, Luo X, Li J. A novel absolute quantitative imaging strategy of iron, copper and zinc in brain tissues by Isotope Dilution Laser Ablation ICP-MS. *Anal Chim Acta.* 2017;984:66–75. <https://doi.org/10.1016/j.aca.2017.07.003>.
- Caceres JO, Pelascini F, Motto-Ros V, Moncayo S, Trichard F, Panczer G, et al. Megapixel multi-elemental imaging by laser-induced breakdown spectroscopy, a technology with considerable potential for paleoclimate studies. *Sci Rep.* 2017;7(1):5080. <https://doi.org/10.1038/s41598-017-05437-3>.
- Fingerhut S, Niehoff AC, Sperling M, Jeibmann A, Paulus W, Niederstadt T, et al. Spatially resolved quantification of gadolinium deposited in the brain of a patient treated with gadolinium-based contrast agents. *J Trace Elements Med Biol: organ of the Society for Minerals and Trace Elements.* 2018;45:125–30. <https://doi.org/10.1016/j.jtemb.2017.10.004>.
- Reifschneider O, Wentker KS, Strobel K, Schmidt R, Masthoff M, Sperling M, et al. Elemental bioimaging of thulium in mouse tissues by laser ablation-ICPMS as a complementary method to heteronuclear proton magnetic resonance imaging for cell tracking experiments. *Anal Chem.* 2015;87(8):4225–30. <https://doi.org/10.1021/ac504363q>.
- Koppen C, Reifschneider O, Castanheira I, Sperling M, Karst U, Ciarimboli G. Quantitative imaging of platinum based on laser ablation-inductively coupled plasma-mass spectrometry to



- investigate toxic side effects of cisplatin. *Metallomics: integrated biometal science*. 2015;7(12):1595–603. <https://doi.org/10.1039/c5mt00226e>.
16. Bartkus L, Amarasiriwardena D, Arriaza B, Bellis D, Yañez J. Exploring lead exposure in ancient Chilean mummies using a single strand of hair by laser ablation-inductively coupled plasma-mass spectrometry (LA-ICP-MS). *Microchem J*. 2011;98(2):267–74. <https://doi.org/10.1016/j.microc.2011.02.008>.
  17. Christensen JR, McBeth JM, Sylvain NJ, Spence J, Chan HM. Hartnell's time machine: 170-year-old nails reveal severe zinc deficiency played a greater role than lead in the demise of the Franklin Expedition. *J Archaeol Sci Rep*. 2016. <https://doi.org/10.1016/j.jasrep.2016.11.042>.
  18. Jimenez-Lamana J, Laborda F, Bolea E, Abad-Alvaro I, Castillo JR, Bianga J, et al. An insight into silver nanoparticles bio-availability in rats. *Metallomics : integrated biometal science*. 2014;6(12):2242–9. <https://doi.org/10.1039/c4mt00200h>.
  19. Zheng L-N, Sang Y-B, Luo R-P, Wang B, Yi F-T, Wang M, et al. Determination of silver nanoparticles in single cells by micro-well trapping and laser ablation ICP-MS determination. *J Anal At Spectrom*. 2019;34(5):915–21. <https://doi.org/10.1039/c8ja00438b>.
  20. Costas-Rodríguez M, Van Acker T, Hastuti AAMB, Devisscher L, Van Campenhout S, Van Vlierberghe H, et al. Laser ablation-inductively coupled plasma-mass spectrometry for quantitative mapping of the copper distribution in liver tissue sections from mice with liver disease induced by common bile duct ligation. *J Anal At Spectrom*. 2017. <https://doi.org/10.1039/c7ja00134g>.
  21. Samanta G, Sharma R, Roychowdhury T, Chakraborti D. Arsenic and other elements in hair, nails, and skin-scales of arsenic victims in West Bengal, India. *Sci Total Environ*. 2004;326(1-3):33–47. <https://doi.org/10.1016/j.scitotenv.2003.12.006>.
  22. Sussulini A, Becker JS. Application of laser microdissection ICP-MS for high resolution elemental mapping in mouse brain tissue: a comparative study with laser ablation ICP-MS. *Talanta*. 2015;132:579–82. <https://doi.org/10.1016/j.talanta.2014.10.001>.
  23. Grün R, Eggins S, Kinsley L, Moseley H, Sambridge M. Laser ablation U-series analysis of fossil bones and teeth. *Palaeogeogr Palaeoclimatol Palaeoecol*. 2014;416:150–67. <https://doi.org/10.1016/j.palaeo.2014.07.023>.
  24. Stadlbauer C, Reiter C, Patzak B, Stingeder G, Prohaska T. History of individuals of the 18th/19th centuries stored in bones, teeth, and hair analyzed by LA-ICP-MS—a step in attempts to confirm the authenticity of Mozart's skull. *Anal Bioanal Chem*. 2007;388(3):593–602. <https://doi.org/10.1007/s00216-007-1266-3>.
  25. Singh VK, Kumar V, Sharma J. Importance of laser-induced breakdown spectroscopy for hard tissues (bone, teeth) and other calcified tissue materials. *Lasers Med Sci*. 2015;30(6):1763–78. <https://doi.org/10.1007/s10103-014-1549-9>.
  26. Praamsma ML, Parsons PJ. Characterization of calcified reference materials for assessing the reliability of manganese determinations in teeth and bone. *J Anal At Spectrom*. 2014;29(7):1243–51. <https://doi.org/10.1039/c4ja00049h>.
  27. Martinez M, Bayne C, Aiello D, Julian M, Gaume R, Baudelet M. Multi-elemental matrix-matched calcium hydroxyapatite reference materials for laser ablation: evaluation on teeth by laser-induced breakdown spectroscopy. *Spectrochim Acta Part B: Atomic Spectroscopy*. 2019;159:105650. <https://doi.org/10.1016/j.sab.2019.105650>.
  28. Praamsma ML, Parsons PJ. Calibration strategies for quantifying the Mn content of tooth and bone samples by LA-ICP-MS. *Accred Qual Assur*. 2016;21(6):385–93. <https://doi.org/10.1007/s00769-016-1234-8>.
  29. Horner NS, Beauchemin D. The use of sol-gels as solid calibration standards for the analysis of soil samples by laser ablation coupled to inductively coupled plasma mass spectrometry. *J Anal At Spectrom*. 2014;29(4):715–20. <https://doi.org/10.1039/C3JA50374G>.
  30. Narukawa T, Willie S. Dried deposits of biological tissues solubilized using formic acid for LA ICP-TOF-MS. *J Anal At Spectrom*. 2010;25(7):1145. <https://doi.org/10.1039/b927309c>.
  31. Pofízká P, Klus J, Hrdlička A, Vrábek J, Škarková P, Prochazka D, et al. Impact of laser-induced breakdown spectroscopy data normalization on multivariate classification accuracy. *J Anal At Spectrom*. 2017;32(2):277–88. <https://doi.org/10.1039/c6ja00322b>.
  32. Lee Y, Nam S-H, Ham K-S, Gonzalez J, Oropeza D, Quarles D, et al. Multivariate classification of edible salts: simultaneous laser-induced breakdown spectroscopy and laser-ablation inductively coupled plasma mass spectrometry analysis. *Spectrochim Acta Part B: Atomic Spectroscopy*. 2016;118:102–11. <https://doi.org/10.1016/j.sab.2016.02.019>.
  33. Putnam RA, Mohaidat QI, Daabous A, Rehse SJ. A comparison of multivariate analysis techniques and variable selection strategies in a laser-induced breakdown spectroscopy bacterial classification. *Spectrochim Acta Part B: Atomic Spectroscopy*. 2013;87(0):161–7. <https://doi.org/10.1016/j.sab.2013.05.014>.
  34. IUPAC (2014) Compendium of Chemical Terminology “Gold Book” 2nd Edition.
  35. Monk SM, Lev SM. Toxicological applications of cryogenic laser ablation inductively coupled plasma time of flight mass spectrometry (CLA-ICP-TOF-MS). *J Anal At Spectrom*. 2013;28(2):274–9. <https://doi.org/10.1039/c2ja30218g>.
  36. Wagner B, Syta O, Kępa L, Bulska E, Segal I, Halicz L (2018) Evaluation of the role of matrix matching for LA-ICP-MS calibration approaches in quantitative elemental analysis of tooth enamel. *J Mex Chem Soc* 62(2). <https://doi.org/10.29356/jmcs.v62i2.410>
  37. Kasem MA, Gonzalez JJ, Russo RE, Harith MA. Effect of the wavelength on laser induced breakdown spectrometric analysis of archaeological bone. *Spectrochim Acta Part B: Atomic Spectroscopy*. 2014;101:26–31. <https://doi.org/10.1016/j.sab.2014.07.010>.
  38. Noel M, Christensen JR, Spence J, Robbins CT. Using laser ablation inductively coupled plasma mass spectrometry (LA-ICP-MS) to characterize copper, zinc and mercury along grizzly bear hair providing estimate of diet. *Sci Total Environ*. 2015;529:1–9. <https://doi.org/10.1016/j.scitotenv.2015.05.004>.
  39. Gallagher CP, Howland KL, Sandstrom SJ, Halden NM. Migration tactics affect spawning frequency in an iteroparous salmonid (*Salvelinus malma*) from the Arctic. *PLoS One*. 2018;13(12):e0210202. <https://doi.org/10.1371/journal.pone.0210202>.
  40. Warburton ML, Reid MR, Stirling CH, Closs G. Validation of depth-profiling LA-ICP-MS in otolith applications. *Can J Fish Aquat Sci*. 2017;74(4):572–81. <https://doi.org/10.1139/cjfas-2016-0063>.
  41. Grottoli AG, Matthews KA, Palardy JE, McDonough WF. High resolution coral Cd measurements using LA-ICP-MS and ID-ICP-MS: Calibration and interpretation. *Chem Geol*. 2013;356:151–9. <https://doi.org/10.1016/j.chemgeo.2013.08.024>.
  42. Ahmed I, Ahmed R, Yang J, Law AWL, Zhang Y, Lau C. Elemental analysis of the thyroid by laser induced breakdown spectroscopy. *Biomed Opt Express*. 2017;8(11):4865–71. <https://doi.org/10.1364/BOE.8.004865>.
  43. Bellis DJ, Santamaria-Fernandez R. Ink jet patterns as model samples for the development of LA-ICP-SFMS methodology for mapping of elemental distribution with reference to biological samples. *J Anal At Spectrom*. 2010;25(7):957. <https://doi.org/10.1039/b926430b>.
  44. Bonta M, Lohninger H, Marchetti-Deschmann M, Limbeck A. Application of gold thin-films for internal standardization in LA-ICP-MS imaging experiments. *Analyst*. 2014;139(6):1521–31. <https://doi.org/10.1039/c3an01511d>.

45. Stark HJ, Wennrich R. A new approach for calibration of laser ablation inductively coupled plasma mass spectrometry using thin layers of spiked agarose gels as references. *Anal Bioanal Chem.* 2011;399(6):2211–7. <https://doi.org/10.1007/s00216-010-4413-1>.
46. Turková S, Vašínová Galiová M, Štůlová K, Čádková Z, Száková J, Otruba V, et al. Study of metal accumulation in tapeworm section using laser ablation-inductively coupled plasma-mass spectrometry (LA-ICP-MS). *Microchem J.* 2017;133:380–90. <https://doi.org/10.1016/j.microc.2017.04.005>.
47. Izmer A, Gholap D, De Houwer K, Cuyckens F, Vanhaecke F. A pilot study on the use of laser ablation-ICP-mass spectrometry for assessing/mapping the distribution of a drug and its metabolites across the body compartments of rats. *J Anal At Spectrom.* 2012;27(3):413. <https://doi.org/10.1039/c2ja10343e>.
48. Gholap D, Verhulst J, Ceelen W, Vanhaecke F. Use of pneumatic nebulization and laser ablation-inductively coupled plasma-mass spectrometry to study the distribution and bioavailability of an intraperitoneally administered Pt-containing chemotherapeutic drug. *Anal Bioanal Chem.* 2012;402(6):2121–9. <https://doi.org/10.1007/s00216-011-5654-3>.
49. Niehaus R, Sperling M, Karst U. Study on aerosol characteristics and fractionation effects of organic standard materials for bioimaging by means of LA-ICP-MS. *J Anal At Spectrom.* 2015;30(10):2056–65. <https://doi.org/10.1039/c5ja00221d>.
50. Reifschneider O, Wehe CA, Diebold K, Becker C, Sperling M, Karst U. Elemental bioimaging of haematoxylin and eosin-stained tissues by laser ablation ICP-MS. *J Anal At Spectrom.* 2013;28(7):989. <https://doi.org/10.1039/c3ja50046b>.
51. Sancey L, Motto-Ros V, Busser B, Kotb S, Benoit JM, Piednoir A, et al. Laser spectrometry for multi-elemental imaging of biological tissues. *Sci Rep.* 2014;4:6065. <https://doi.org/10.1038/srep06065>.
52. Cheajesadagul P, Wanankul W, Siripinyanon A, Shiowatana J. Metal doped keratin film standard for LA-ICP-MS determination of lead in hair samples. *J Anal At Spectrom.* 2011;26(3):493–8. <https://doi.org/10.1039/c0ja00082e>.
53. Ugarte A, Unceta N, Pécuyer C, Goicolea MA, Barrio RJ. Development of matrix-matching hydroxyapatite calibration standards for quantitative multi-element LA-ICP-MS analysis: application to the dorsal spine of fish. *J Anal At Spectrom.* 2011;26(7):1421. <https://doi.org/10.1039/c1ja10037h>.
54. Singh VK, Rai AK, Rai PK, Jindal PK. Cross-sectional study of kidney stones by laser-induced breakdown spectroscopy. *Lasers Med Sci.* 2009;24(5):749–59. <https://doi.org/10.1007/s10103-008-0635-2>.
55. Bishop DP, Clases D, Fryer F, Williams E, Wilkins S, Hare DJ, et al. Elemental bio-imaging using laser ablation-triple quadrupole-ICP-MS. *J Anal At Spectrom.* 2016;31(1):197–202. <https://doi.org/10.1039/c5ja00293a>.
56. González-Iglesias H, Petrash C, Rodríguez-Menéndez S, García M, Álvarez L, Fernández-Vega Cueto L, et al. Quantitative distribution of Zn, Fe and Cu in the human lens and study of the Zn–metallothionein redox system in cultured lens epithelial cells by elemental MS. *J Anal At Spectrom.* 2017. <https://doi.org/10.1039/c6ja00431h>.
57. Ahmed I, Yang J, Law AWL, Manno FAM, Ahmed R, Zhang Y, et al. Rapid and in situ optical detection of trace lithium in tissues. *Biomed Opt Express.* 2018;9(9):4459–71. <https://doi.org/10.1364/BOE.9.004459>.
58. Reifschneider O, Wehe CA, Raj I, Ehmcke J, Ciarimboli G, Sperling M, et al. Quantitative bioimaging of platinum in polymer embedded mouse organs using laser ablation ICP-MS. *Metalomics : integrated biometal science.* 2013;5(10):1440–7. <https://doi.org/10.1039/c3mt00147d>.
59. Eastman RR, Jursa TP, Benedetti C, Lucchini RG, Smith DR. Hair as a biomarker of environmental manganese exposure. *Environ Sci Technol.* 2013;47(3):1629–37. <https://doi.org/10.1021/es3035297>.
60. Dressler VL, Pozebon D, Mesko MF, Matusch A, Kumtabtim U, Wu B, et al. Biomonitoring of essential and toxic metals in single hair using on-line solution-based calibration in laser ablation inductively coupled plasma mass spectrometry. *Talanta.* 2010;82(5):1770–7. <https://doi.org/10.1016/j.talanta.2010.07.065>.
61. Pozebon D, Dressler VL, Matusch A, Becker JS. Monitoring of platinum in a single hair by laser ablation inductively coupled plasma mass spectrometry (LA-ICP-MS) after cisplatin treatment for cancer. *Int J Mass Spectrom.* 2008;272(1):57–62. <https://doi.org/10.1016/j.ijms.2008.01.001>.
62. Byrne S, Amarasiriwardena D, Bandak B, Bartkus L, Kane J, Jones J, et al. Were Chinchorros exposed to arsenic? Arsenic determination in Chinchorro mummies' hair by laser ablation inductively coupled plasma-mass spectrometry (LA-ICP-MS). *Microchem J.* 2010;94(1):28–35. <https://doi.org/10.1016/j.microc.2009.08.006>.
63. Steely S, Amarasiriwardena D, Jones J, Yañez J. A rapid approach for assessment of arsenic exposure by elemental analysis of single strand of hair using laser ablation-inductively coupled plasma-mass spectrometry. *Microchem J.* 2007;86(2):235–40. <https://doi.org/10.1016/j.microc.2007.03.009>.
64. Barats A, Pécuyer C, Amouroux D, Dubascoux S, Chauvaud L, Donard OF. Matrix-matched quantitative analysis of trace-elements in calcium carbonate shells by laser-ablation ICP-MS: application to the determination of daily scale profiles in scallop shell (*Pecten maximus*). *Anal Bioanal Chem.* 2007;387(3):1131–40. <https://doi.org/10.1007/s00216-006-0954-8>.
65. Draxler J, Zitek A, Meischel M, Stranzl-Tschegg SE, Mingler B, Martinelli E, et al. Regionalized quantitative LA-ICP-MS imaging of the biodegradation of magnesium alloys in bone tissue. *J Anal At Spectrom.* 2015;30(12):2459–68. <https://doi.org/10.1039/c5ja00354g>.
66. Gruhl S, Witte F, Vogt J, Vogt C. Determination of concentration gradients in bone tissue generated by a biologically degradable magnesium implant. *J Anal At Spectrom.* 2009;24(2):181–8. <https://doi.org/10.1039/b813734j>.
67. Balter V, Lécuyer C. Determination of Sr and Ba partition coefficients between apatite and water from 5°C to 60°C: a potential new thermometer for aquatic paleoenvironments 1 | Associate editor: A. Mucci *Geochim Cosmochim Acta.* 2004;68(3):423–32. [https://doi.org/10.1016/S0016-7037\(03\)00453-8](https://doi.org/10.1016/S0016-7037(03)00453-8).
68. Tacaíl T, Télouk P, Balter V. Precise analysis of calcium stable isotope variations in biological apatites using laser ablation MC-ICPMS. *J Anal At Spectrom.* 2016;31(1):152–62. <https://doi.org/10.1039/c5ja00239g>.
69. Miliszkiwicz N, Walas S, Tobiasz A, Kołodziej M, Szostek K. Calibration for elemental dental tissue analysis by laser ablation inductively coupled plasma mass spectrometry. *Anal Lett.* 2016;50(8):1345–59. <https://doi.org/10.1080/00032719.2016.1225305>.
70. Sutharsini U, Thanishaichelvan M, Singh R. Two-step sintering of ceramics. 2018. <https://doi.org/10.5772/68083>.

**Publisher's note** Springer Nature remains neutral with regard to jurisdictional claims in published maps and institutional affiliations.

Springer Nature or its licensor (e.g. a society or other partner) holds exclusive rights to this article under a publishing agreement with the author(s) or other rightsholder(s); author self-archiving of the accepted manuscript version of this article is solely governed by the terms of such publishing agreement and applicable law.